IscA, an Alternate Scaffold for Fe−S Cluster Biosynthesis†

Carsten Krebs,‡ Jeffrey N. Agar,§,|| Archer D. Smith,§ Jeverson Frazzon,⊥ Dennis R. Dean,*,⊥ Boi Hanh Huynh,*,‡ and Michael K. Johnson*,§

Department of Physics, Emory University, Atlanta, Georgia 30322, Department of Chemistry and Center for Metalloenzyme Studies, University of Georgia, Athens, Georgia 30602, and Department of Biochemistry, Virginia Tech, Blacksburg, Virginia 24061

Received August 8, 2001; Revised Manuscript Received September 25, 2001

ABSTRACT: An IscA homologue within the *nif* regulon of *Azotobacter vinelandii*, designated ^{Nif}IscA, was expressed in *Escherichia coli* and purified to homogeneity. Purified ^{Nif}IscA was found to be a homodimer of 11-kDa subunits that contained no metal centers or other prosthetic groups in its as-isolated form. Possible roles for ^{Nif}IscA in Fe−S cluster biosynthesis were assessed by investigating the ability to bind iron and to assemble Fe−S clusters in a NifS-directed process, as monitored by the combination of UV−vis absorption, Mössbauer, resonance Raman, variable-temperature magnetic circular dichroism, and EPR spectroscopies. Although ^{Nif}IscA was found to bind ferrous ion in a tetrahedral, predominantly cysteinyl-ligated coordination environment, the low-binding affinity argues against a specific role as a metallochaperone for the delivery of ferrous ion to other Fe−S cluster assembly proteins. Rather, a role for ^{Nif}IscA as an alternate scaffold protein for Fe−S cluster biosynthesis is proposed, based on the NifS-directed assembly of approximately one labile $[4Fe\text{-}4S]^{2+}$ cluster per ^{Nif}IscA homodimer, via a transient $[2Fe\text{-}2S]^{2+}$ cluster intermediate. The cluster assembly process was monitored temporally using UV−vis absorption and Mössbauer spectroscopy, and the intermediate $[2Fe\text{-}2S]^{2+}$-containing species was additionally characterized by resonance Raman spectroscopy. The Mössbauer and resonance Raman properties of the $[2Fe\text{-}2S]^{2+}$ center are consistent with complete cysteinyl ligation. The presence of three conserved cysteine residues in all IscA proteins and the observed cluster stoichiometry of approximately one $[2Fe\text{-}2S]^{2+}$ or one $[4Fe\text{-}4S]^{2+}$ per homodimer suggest that both cluster types are subunit bridging. In addition, ^{Nif}IscA was shown to couple delivery of iron and sulfur by using ferrous ion to reduce sulfane sulfur. The ability of Fe−S scaffold proteins to couple the delivery of these two toxic and reactive Fe−S cluster precursors is likely to be important for minimizing the cellular concentrations of free ferrous and sulfide ions. On the basis of the spectroscopic and analytical results, mechanistic schemes for NifS-directed cluster assembly on ^{Nif}IscA are proposed. It is proposed that the IscA family of proteins provide alternative scaffolds to the NifU and IscU proteins for mediating *nif*-specific and general Fe−S cluster assembly.

Biological Fe−S clusters are among the most ancient, ubiquitous, and functionally diverse prosthetic groups in all of biology (for recent reviews, see refs *1*−*5*). There are now known to be in excess of 120 distinct types of Fe−S-cluster-containing enzymes and proteins, with [2Fe-2S] and cubane-type [3Fe-4S] and [4Fe-4S] units constituting the most common structural motifs. While Fe−S-containing proteins have been the focus of extensive genetic, biochemical, and biophysical characterization, information on the complex process of cluster biosynthesis has only recently begun to emerge. Much of the current understanding of cluster biosynthesis originated from studies of the organization and function of nitrogen fixing (*nif*) genes in the aerobic nitrogen-fixing bacterium *Azotobacter vinelandii*. Two gene products, NifS and NifU, were found to be essential for optimal assembly of Fe−S clusters in the nitrogenase proteins (*6*, *7*). Subsequent studies revealed that NifS is a homodimeric, pyridoxal phosphate-dependent L-cysteine desulfurase that catalyzes the conversion of cysteine to alanine and sulfane sulfur via a protein-bound cysteine persulfide intermediate (*8*, *9*). NifU was shown to be a homodimeric protein containing a redox-active $[2Fe\text{-}2S]^{2+,+}$ cluster (*10*) and an additional site that serves as a scaffold for NifS-directed assembly of a transient cluster (*11*, *12*).

Homologues of *nifU* and *nifS*, termed *iscU* and *iscS*, respectively, were subsequently identified in *A. vinelandii* and *Escherichia coli* (*13*) and found to be part of a widely conserved prokaryotic operon involved with general iron−sulfur cluster biosynthesis. IscS was shown to have cysteine desulfurase activity and to be highly homologous to NifS. IscU is a truncated version of NifU, containing only the N-terminal transient-cluster binding domain identified in NifU. In vitro studies have demonstrated that IscU provides

† This work was supported by grants from the National Institutes of Health (GM62524 to M.K.J. and GM47295 to B.H.H.) and the National Science Foundation (MCB9630127 to D.R.D.).

* To whom correspondence should be addressed. (M. K. J.) Phone: (706) 542-9378. Fax: (706) 542-2353. E-mail: johnson@chem.uga.edu. (B.H.H.) Phone (404) 727-4295. Fax: (404) 727-0873. E-mail: vhuynh@emory.edu. (D.R.D.) Phone: (540) 231-5895. Fax: (540) 231-7126. E-mail: deandr@vt.edu.

‡ Emory University.

§ University of Georgia.

|| Current address: Montreal Neurological Institute, 3801 University St., Montreal, PQ H3A 2B4.

⊥ Virginia Tech.

10.1021/bi015656z CCC: $20.00
Published on Web 10/16/2001

a scaffold for sequential, IscS-directed assembly of [2Fe-2S]$^{2+}$ and [4Fe-4S]$^{2+}$ clusters (*14*, *15*). In addition to *iscU* and *iscS*, the *isc* operon contains genes encoding a regulatory protein, IscR,[1] two molecular chaperones, HscA and HscB, a [2Fe-2S] ferredoxin, Fdx, and a highly conserved protein of unknown function termed IscA (*12*, *13*). A homologue of *iscA* (previously termed *orf6*) is also present in the *nif* regulon and is located immediately upstream of *nifU*. The *nif*-specific homologue of IscA, designated ^{Nif}IscA,[2] is the focus of this study. Except for IscR, homologues to all the Isc proteins have also been identified in the mitochondria of eukaryotes (*16*), indicating that the process of Fe−S cluster biosynthesis is highly conserved among many different organisms.

Gene disruption studies in *E. coli* (*17*, *18*) and *Saccharomyces cerevisiae* (*19*−*21*) have demonstrated an important, albeit nonessential, role for IscA-type proteins in Fe−S cluster biosynthesis. Moreover, point mutations in each of the three conserved cysteine residues yield the same phenotypes as the gene knockouts (*19*, *21*). This suggests a role for IscA-type proteins in Fe−S cluster biosynthesis that involves binding of either Fe and/or an Fe−S cluster. To address the role of IscA-type proteins, we report here an investigation into the ability of *A. vinelandii* ^{Nif}IscA to bind Fe and to assemble Fe−S clusters in a NifS-directed process, using the combination of UV−vis absorption, variable-temperature magnetic circular dichroism (VTMCD), resonance Raman and Mössbauer spectroscopies. The results demonstrate that ^{Nif}IscA provides an alternative scaffold to NifU for the NifS-directed sequential assembly of [2Fe-2S]$^{2+}$ and [4Fe-4S]$^{2+}$ clusters and reveal mechanistic insight into the cluster assembly process.

MATERIALS AND METHODS

Purification of ^{Nif}IscA. The *A. vinelandii* ^{Nif}*iscA* gene was amplified using the polymerase chain reaction method and inserted into the expression plasmid PT_7-7, as previously described for the *nifU* (*10*) and *nifS* (*8*) genes. This plasmid, designated pDB570, was transformed into the *Escherichia coli* host BL21(DE3) and induced for high level expression of ^{Nif}IscA, as previously described (*8*) for other similar constructs. For purification of heterologously produced ^{Nif}IscA, 30 g of cell paste was resuspendend in 60 mL of a 25 mM Tris-HCl buffer (pH7.4) containing 2 mM β-mercaptoethanol. The cells were disrupted using sonication and centrifuged at 25 000 rpm for 20 min using a Beckman Ti45 rotor. All biochemical manipulations were performed with degassed, Argon-purged buffers under anoxic conditions. Solid streptomycin sulfate (1% weight/volume) was added to the crude extract, incubated at room temperature for 5 min, and centrifuged as above. The supernatant fraction was brought to 40% saturation at room temperature with ammonium sulfate, centrifuged as above, and the resulting pellet resuspended in approximately 400 mL of the above buffer. The sample was then loaded on a 2.5 cm × 30 cm Q-sepharose anion-exchange chromatography column and fractionated using a 400 mL 0.7 to 1.0 M NaCl gradient (25 mM Tris-HCl, pH 7.4). The fraction that eluted between 0.42 and 0.49 M NaCl was collected and concentrated to 10 mL using an Amicon ultrafiltration device fitted with a YM10 filter. The concentrated sample was then loaded on a 2.5 cm × 60 cm column packed with a Bio gel P30 size exclusion matrix and eluted with 25 mM Tris-HCl buffer applied to the column at 1 mL/min. This procedure routinely yields approximately 80 mg of ∼95% pure ^{Nif}IscA protein that migrates as a single homogeneous band using denaturing polyacrylamide gel electrophoresis. The native molecular weight for ^{Nif}IscA was determined by gel-filtration chromatography using a 1 cm × 30 cm Superose 6 FPLC column. The elution buffer used for native molecular weight determination was 50 mM Tris-HCl (pH 7.4) and 200 mM KCl, which was applied to the column at a flow rate of 0.3 mL/min. Standards used for native molecular weight determination were alcohol dehydrogenase (M_r 150 000), bovine serum albumin (M_r 66 000), carbonic anhydrase (M_r 29 000), and cytochrome *c* (M_r 12 400). Prior to use for iron binding and cluster assembly experiments, samples of ^{Nif}IscA were treated with 10 mM dithiothreitol (DTT) and then repurified by anion-exchange chromatography and ultrafiltration as described above. All samples of ^{Nif}IscA used in the work were in 50 mM Tris-HCl buffer at pH 7.8.

Chemical Analysis. Protein concentrations were determined using the procedure of Brown et al. (*22*). Iron determinations for total iron were carried out using a modified version of the procedure described by Haigler et al. (*23*). The 10-min incubation at room temperature of protein samples in the presence of 12 M HCl was replaced by a complete sample digestion using of 3:1 HCl:HNO_3 at 80 °C for 1 h followed by addition of 6 M perchloric acid for 30 min. Metal analyses were also carried out using a Thermo Jarrel-Ash 965 inductively coupled argon plasma (ICP) emission spectrometer in the Chemical Analysis Facility at the University of Georgia.

Spectroscopic Methods. Samples for all spectroscopic investigations were prepared under argon in a Vacuum Atmospheres glovebox (<1 ppm O_2). UV−vis absorption spectra were recorded in septum-sealed 1 mm cuvettes, using a Shimadzu 3101 PC scanning spectrophotometer. Resonance Raman spectra were recorded on droplets of frozen protein solutions at 17 K using an Instruments SA Ramanor U1000 scanning spectrometer fitted with a cooled RCA 31034 photomultiplier tube and lines from a Coherent Sabre 10-W argon ion laser (*24*). Signal-to-noise was improved by multiple scans and bands due to the frozen buffer solution were subtracted from all the spectra shown in this work after normalization of lattice modes of ice centered at 229 cm^{-1}. VTMCD spectra were recorded using samples containing 55% (v/v) glycerol in 1 mm cuvettes using an Oxford Instruments Spectromag 4000 (0−7 T) split-coil superconducting magnet (1.5−300 K) mated to a Jasco J-715 spectropolarimeter (*25*, *26*). X-band (∼9.6 GHz) EPR spectra were recorded using a Bruker ESP-300E EPR spectrometer equipped with a dual-mode ER-4116 cavity and an Oxford Instruments ESR-9 flow cryostat. Mössbauer spectra in the presence of weak and strong applied magnetic fields were recorded using the previously described instrumentation (*27*). Analysis of the Mössbauer data was performed with the program WMOSS (Web Research).

[1] Patricia J, Kiley, personal communication, and unpublished results from the laboratory of Dennis R. Dean.

[2] Abbreviations: ^{Nif}IscA, gene product of *nif*-specific *iscA*; VTMCD, variable-temperature magnetic circular dichroism; DTT, dithiothreitol.

NifS-Directed Fe−S Cluster Assembly on ^{Nif}IscA. The concentrations of NifS, ^{Nif}IscA, ferrous sulfate, and cysteine were kept constant at 15 μM, 0.5 mM, 2 mM, and 8 mM, respectively. The protein concentrations refer to the concentrations of ^{Nif}IscA and NifS monomers, and the buffer used was 50 mM Tris-HCl at pH 7.8. For the preparation of Mössbauer samples, ^{57}Fe-enriched ferrous sulfate was used (>95% enrichment). Cluster assembly on ^{Nif}IscA was performed at room temperature under argon in a Vacuum Atmospheres glovebox. For the time-based spectroscopic studies, the first sample was frozen 2 min after all the reactants were mixed together. The frozen samples were then subjected to spectroscopic measurements, followed by thawing the samples to room temperature and incubating for a given time before refreezing for measurements at the next time point. The total number of freeze−thaw cycles on a given sample did not exceed five. The effect of freeze−thaw cycles on the reaction was examined by UV−vis absorption spectroscopy and was found to be negligible: UV−vis absorption spectroscopy of reaction mixtures which had been frozen and thawed at six different reaction times and allowed to continue reacting showed no quantitative or qualitative difference from those of mixtures that were never frozen. Attempts to resolve discrete ^{Nif}IscA fractions from the reaction mixture were carried out inside the glovebox using a Pharmacia FPLC with a 5-mL High-Trap Q-Sepharose column (Pharmacia).

RESULTS

Purification and Biochemical Characterization of ^{Nif}IscA. ^{Nif}IscA was cloned, expressed in *E. coli*, and purified to homogeneity as judged by denaturing gel electrophoresis and UV absorption. Purified samples of *A. vinelandii* ^{Nif}IscA were colorless and contained no significant amount of any metal ion as judged by ICP emission spectroscopy. The UV absorption comprises maxima at 260 nm (ϵ = 1.72 mM^{-1} cm^{-1}), 267 nm (ϵ = 1.72 mM^{-1} cm^{-1}), and 276 nm (ϵ = 1.65 mM^{-1} cm^{-1}) with a pronounced shoulder at 284 nm (Figure 1, broken line) and the extinction coefficients are in excellent agreement with those predicted from the primary sequence. ^{Nif}IscA eluted as a single homogeneous peak from gel-filtration columns with an apparent native molecular weight of 22 500. Since the monomer molecular weight is 11 047, based on the primary sequence, this behavior indicates that ^{Nif}IscA is a dimer in solution.

^{Nif}IscA Iron Binding. The possibility that IscA is involved in mediating delivery of iron for Fe−S cluster biosynthesis was assessed by investigating the ability of ^{Nif}IscA to bind ferrous or ferric ion as monitored by UV−vis absorption spectroscopy coupled with parallel VTMCD or Mössbauer studies. The combination of these spectroscopic techniques is particularly effective in detecting, identifying and quantifying cysteinyl-ligated, high-spin, mononuclear Fe(II) or Fe(III) species (*28*−*30*). In the absence of exogenous DTT, no spectroscopic evidence for Fe^{3+} binding to the cysteinyl residues of ^{Nif}IscA was obtained, on addition of up to a 10-fold excess of ferric citrate. However, all three spectroscopic techniques afforded evidence for weak binding of ferrous ion in a predominantly cysteinyl-ligated tetrahedral coordination environment.

The first indication that ^{Nif}IscA is able to bind ferrous ion came from UV−vis absorption studies of samples treated with an up to 4-fold stoichiometric excess of ferrous sulfate per ^{Nif}IscA monomer. Addition of ferrous sulfate results in the appearance of a band centered at 315 nm, with a high-energy shoulder centered near 340 nm (Figure 1A). These absorption bands correlate with temperature-dependent MCD bands: positive band centered at 335 nm and negative band centered at 305 nm with a shoulder at ~280 nm (Figure 1B). Both the absorption and VTMCD spectra are very similar to those observed for reduced rubredoxin and metallothionein with <4 equiv of Fe(II) bound (*28*) and are attributed to charge transfer transitions associated with a tetrahedrally coordinated high-spin (S = 2) Fe(II) center with cysteinate ligation. Since rubredoxin variants with one coordinating cysteine replaced by aspartate can give rise to analogous absorption and VTMCD spectra (*31*), the spectra are consistent with tetrahedral coordination involving four cysteinate ligands or three cysteinate and one oxygenic ligand. However, the maximum absorption and MCD extinction coefficients are less than 20% of those determined per tetrahedral Fe(II) center in wild-type and variant rubredoxins and in metallothionein under analogous conditions (*28*, *31*), indicating substoichiometric ferrous binding to ^{Nif}IscA. This is further supported by Mössbauer-monitored ^{Nif}IscA ferrous titrations in which 0.25, 0.50, 1.0, 2.0, and 4.0 equiv of $^{57}FeSO_4$ were added per ^{Nif}IscA monomer. The Mössbauer spectra are dominated by the broad quadrupole doublet (δ

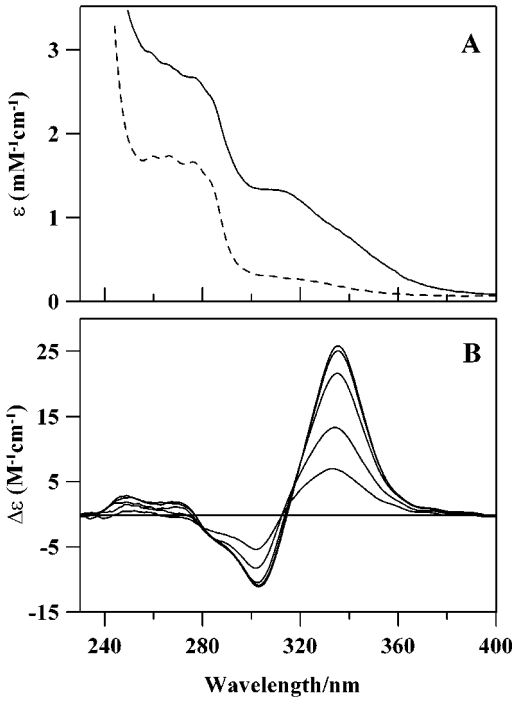

FIGURE 1: UV−vis absorption and VTMCD spectra of *A. vinelandii* ^{Nif}IscA in the presence of excess ferrous sulfate. (A) Absorption spectra. Broken line is ^{Nif}IscA treated with 10 mM DTT and then repurified and concentrated anaerobically by anion-exchange chromatography and ultrafiltration. Solid line is DTT-treated ^{Nif}IscA (0.1 mM) incubated at room temperature for 10 min with a 4-fold stoichiometric excess of ferrous sulfate. The absorption spectrum of excess ferrous sulfate has been subtracted from the spectrum shown. (B) VTMCD spectra of ferrous-bound ^{Nif}IscA. Sample was prepared by incubating 0.6 mM ^{Nif}IscA with a 10-fold excess of ferrous sulfate followed by exchange into the equivalent D_2O buffer via ultrafiltration. After addition of 55% (v/v) d_3-glycerol, the sample was 2.6 mM in ^{Nif}IscA. MCD spectra recorded at 6 T at 1.8, 4.3, 10.3, 24.5, and 52.5 K. All bands increase in intensity with decreasing temperature.

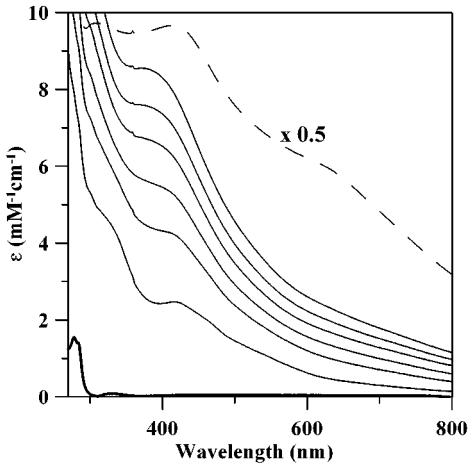

FIGURE 2: NifS-catalyzed assembly of Fe−S clusters on ^{Nif}IscA monitored by UV−vis absorption spectroscopy. Protein and reagent concentrations are described in the Materials and Methods. Thick solid line, ^{Nif}IscA as-isolated. Thin solid lines from bottom to top, 10, 20, 30, 40, 50, and 60 min after initiation of NifS-catalyzed Fe−S cluster assembly. Broken line, 2 h after initiation of NifS-catalyzed Fe−S cluster assembly; absorption intensity divided by two compared to other time points.

$= 1.2$ mm/s and $\Delta E_Q = 3.2$ mm/s) that is commonly observed for aqueous ferrous species. Evidence for ferrous binding in a predominantly cysteinyl-ligated tetrahedral coordination environment is manifested by a poorly resolved quadrupole doublet with $\delta = 0.7$ mm/s and $\Delta E_Q = 3.3$ mm/s which maximally corresponds to 0.25 Fe/^{Nif}IscA monomer (data not shown). The spectroscopic features associated with the ferrous-bound form of ^{Nif}IscA were lost on removal of excess aqueous ferrous ion by gel filtration. Overall, the spectroscopic data indicate that ferrous can bind to ^{Nif}IscA in a tetrahedral predominantly cysteinyl-ligated coordination environment. However, the binding is weak with at least a 10-fold stoichiometric excess of ferrous ion required to achieve 50% binding.

Time Course of NifS Catalyzed Fe−S Cluster Assembly on ^{Nif}IscA. The addition of cysteine and a catalytic amount of NifS to a mixture of ferrous sulfate and ^{Nif}IscA was monitored as a function of time using UV−vis absorption (Figure 2). Catalytic rather than stoichiometric amounts of NifS were used in order to slow the reaction down and thereby facilitate spectroscopic characterization of the time course. The initial visible absorption spectrum after 10 min comprises a pronounced shoulder centered at 320 nm and a band at 415 nm with low-energy shoulders centered at ~460 and ~540 nm and is indicative of the formation of a $[2Fe\text{-}2S]^{2+}$ cluster (*14*, *32*). The absorption intensity increases with increasing time and this is accompanied by a blue shift in the 415-nm band. After 60 min, the spectrum comprises bands at 320 and 390 nm, which is more characteristic of a $[4Fe\text{-}4S]^{2+}$ cluster (*15*). If the reaction is allowed to proceed for an additional 60 min, the absorption intensity continues to increase and the band at 390 nm red shifts to 420 nm concomitant with the appearance of an intense shoulder centered around 600 nm. The resultant spectrum after 2 h is indicative of soluble, protein-free, polymeric iron-sulfides, which is the sole product observed in controls with ^{Nif}IscA omitted from the reaction mixture. Difference spectroscopy indicates that the polymeric iron-sulfides start to accumulate primarily after the formation of $[2Fe\text{-}2S]^{2+}$ and $[4Fe\text{-}4S]^{2+}$ clusters on ^{Nif}IscA. The same soluble polymeric iron-sulfide species is also observed after completion of NifS- or IscS-catalyzed cluster assembly on NifU and IscU, respectively (*11*, *15*).

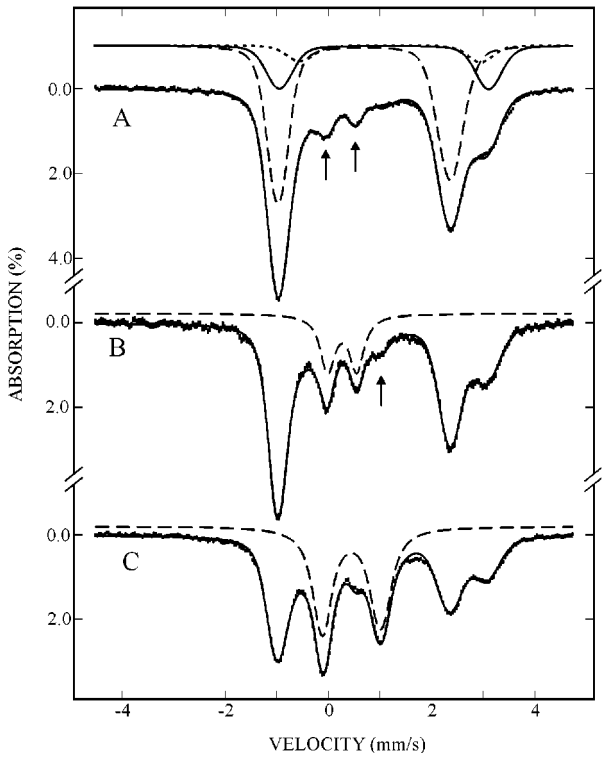

FIGURE 3: Time-dependent Mössbauer spectra of NifS-catalyzed assembly of Fe−S clusters on ^{Nif}IscA. The reaction mixture (see Materials and Methods) was frozen at reaction times of (A) 2 min, (B) 12 min, and (C) 40 min. The spectra (hashed marks) were recorded at 4.2 K in a magnetic field of 50 mT applied parallel to the γ radiation. The solid lines overlaid with the experimental spectra are theoretical simulations using the parameters listed in Tables 1 and 2. Simulations for the individual Fe(II) species are shown above spectrum A: $Fe^{II}Cys_4$, dashed line; Fe^{II}-3.5, dotted line; Fe^{II}-4.1, solid line. Simulations for the $[2Fe\text{-}2S]^{2+}$ cluster and $[4Fe\text{-}4S]^{2+}$ cluster are shown as dashed lines in panels B and C, respectively. Arrows in panels A mark the peak positions of the spectrum of the $[2Fe\text{-}2S]^{2+}$ cluster and the arrow in panels B marks the high-energy line position of the spectrum of the $[4Fe\text{-}4S]^{2+}$ cluster.

To characterize further the sequence of events that occur during NifS-catalyzed cluster assembly on ^{Nif}IscA, Mössbauer spectroscopy was used to monitor the changing states of the iron in the reaction mixture as a function of reaction time. The reaction was initiated by addition of cysteine to a solution containing ^{Nif}IscA, NifS, and $^{57}FeSO_4$. The solution was split into two fractions; one was frozen for Mössbauer investigation and the other was used for parallel UV−vis measurements (see Materials and Methods). After completion of the Mössbauer measurements, the sample was thawed to room temperature and the reaction was allowed to proceed for a preselected period of time, before refreezing for further studies. This procedure was repeated several times until the assembly process was completed (i.e., no more Fe−S clusters are generated), which takes about 40−45 min. The entire time-based Mössbauer study was duplicated once and the results were in good agreement.

Figure 3 shows the time-dependent Mössbauer spectra of one sample that was frozen at reaction times of 2 min (A), 12 min (B), and 40 min (C). The data were recorded at 4.2

Table 1: Mössbauer Parameters of the Fe Species Detected during Assembly of Fe−S Cluster on ^{Nif}IscA

Fe species	(δ mm/s)	ΔE_Q (mm/s)
$Fe^{II}cys_4$	0.69 ± 0.02	3.34 ± 0.05
Fe^{II}-3.5	1.18 ± 0.02	3.6 ± 0.05
Fe^{II}-4.1	1.08 ± 0.02	4.05 ± 0.05
$[2Fe\text{-}2S]^{2+}$	0.26 ± 0.02	0.55 ± 0.02
$[4Fe\text{-}4S]^{2+}$		
site 1	0.46 ± 0.02	1.25 ± 0.05
site 2	0.44 ± 0.02	1.04 ± 0.05

Table 2: Percent Mössbauer Absorptions of the Fe Species Detected during Assembly of Fe−S Cluster in ^{Nif}IscA as a Function of Reaction Time

reaction time (min)	$Fe^{II}cys_4$	Fe^{II}-3.5	Fe^{II}-4.1	$[2Fe\text{-}2S]^{2+}$	$[4Fe\text{-}4S]^{2+}$
2	59 ± 4	7 ± 4	19 ± 4	10 ± 2	5 ± 2
12	47 ± 4	7 ± 4	18 ± 4	18 ± 2	9 ± 2
25	35 ± 4	6 ± 4	16 ± 4	10 ± 2	34 ± 2
40	30 ± 4	5 ± 4	13 ± 4	9 ± 2	42 ± 2

K in a magnetic field of 50 mT, applied parallel to the γ radiation. Global analysis of the data indicates that the entire set of data can be deconvoluted into five spectral components. On the basis of their Mössbauer parameters, three components are assigned to high-spin Fe(II) species, one to a $[2Fe\text{-}2S]^{2+}$ cluster, and one to $[4Fe\text{-}4S]^{2+}$ cluster. The Mössbauer parameters of these five Fe species obtained from the global analysis are listed in Table 1, and their relative absorption intensities as a function of reaction time are listed in Table 2. The solid lines overlaid with the experimental spectra shown in Figure 3 are theoretical simulations using the results of the global analysis. The agreement between experiment and theory is satisfactory.

Near the start of the reaction (e.g., at 2 min reaction time), the majority of the Fe is present as high-spin ferrous ions (Figure 3A). Analysis of the data indicates that at least three high-spin Fe(II) species are required in order to explain the Mössbauer absorption features observed at the region between 2 and 4 mm/s. One of the Fe(II) species exhibits a quadrupole doublet (dashed line plotted above the spectrum shown in Figure 2A) with parameters (δ = 0.70 mm/s and ΔE_Q = 3.3 mm/s) that are typical for tetrahedral sulfur coordination and is therefore assigned to an $Fe^{II}Cys_4$ species (*30*). The other two Fe(II) species show larger isomer shifts (δ_1 = 1.19 mm/s and δ_2 = 1.08 mm/s) and quadrupole splittings (ΔE_{Q1} = 3.5 mm/s and ΔE_{Q2} = 4.1 mm/s) and are labeled according to their ΔE_Q parameters, Fe^{II}-3.5 and Fe^{II}-4.1, respectively. The spectra of Fe^{II}-3.5 and Fe^{II}-4.1 are also shown above the spectrum in Figure 3A as a dotted and solid line, respectively. For the Fe^{II}-3.5 species, the parameters are consistent with a coordination of five or six N/O donors (*33*, *34*). The smaller isomer shift of Fe^{II}-4.1 suggests partial S coordination (*35*) and the ΔE_Q is unique and unusually large. The spectra of these two Fe(II) species have large line widths, suggesting the presence of microheterogeneities for these Fe species. However, none of these Fe(II) species are likely to be associated with ^{Nif}IscA. Control experiments using only $^{57}FeSO_4$ and cysteine, i.e., without ^{Nif}IscA and NifS, exhibited the $Fe^{II}Cys_4$, Fe^{II}-3.5, and Fe^{II}-4.1 species in an 8:1:1 ratio (see Supporting Information, Figure S1). Hence, these Fe(II) species appear to reflect the equilibrium concentrations of species formed on reaction of aqueous Fe(II) ion with a 4-fold excess of cysteine.

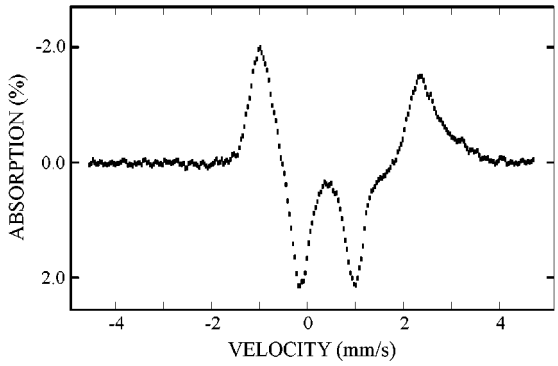

FIGURE 4: Difference Mössbauer spectrum between spectra of the 40- and 2-min samples shown in Figure 3. Conversion of Fe(II) species (negative absorption) to $[4Fe\text{-}4S]^{2+}$ cluster (positive absorption) over the reaction time is clearly demonstrated.

In addition to the major features resulting from the Fe(II) species, the 2-min sample also shows two weak absorption peaks (marked by arrows) at the central region of its spectrum. Analysis of the data indicates that these two peaks arise from a $[2Fe\text{-}2S]^{2+}$ cluster and thus reveals the early formation of a [2Fe-2S] cluster at the start of the cluster assembly process. With longer reaction time, the accumulation of the $[2Fe\text{-}2S]^{2+}$ cluster increases, and at 12 min (Figure 3B), approximately 17.5% of the iron absorption can be attributed to the $[2Fe\text{-}2S]^{2+}$ cluster (dashed line plotted above the experimental spectrum shown in Figure 3B), which corresponds to approximately 0.35 clusters per ^{Nif}IscA monomer. Interestingly, the spectrum of the 12-min sample shows the appearance of a small peak at ~1 mm/s (marked by an arrow), which can be attributed to a $[4Fe\text{-}4S]^{2+}$ cluster. After reacting for 40 min, the accumulation of $[2Fe\text{-}2S]^{2+}$ cluster decreases to a level below that of the 2-min sample, indicating that the $[2Fe\text{-}2S]^{2+}$ cluster is a transient species in the cluster assembly process. On the other hand, the accumulation of $[4Fe\text{-}4S]^{2+}$ clusters increases with increasing reaction time, and at 40 min (Figure 3C), it reaches a level that accounts for 42% of the total iron absorption (dashed line plotted above the experimental spectrum shown in Figure 3C), or approximately 0.8 cluster/^{Nif}IscA dimer. Comparing the experimental data (Figure 3 and Table 2) of the 40- and 2-min samples, it can be seen that the increase in absorption intensity of the $[4Fe\text{-}4S]^{2+}$ cluster is compensated by the decrease in intensity of the three Fe(II) species, with the $Fe^{II}Cys_4$ species accounting for most of the lost intensity. To illustrate this point, a difference spectrum between the spectra of the 2- and 40-min samples is shown in Figure 4. The upward pointing peaks (negative absorption) coincide with those of the Fe(II) species and the downward pointing peaks (positive absorption) are identical to those of the $[4Fe\text{-}4S]^{2+}$ cluster. This difference spectrum thus establishes unambiguously the conversion of the Fe(II) species to the $[4Fe\text{-}4S]^{2+}$ cluster assembled on ^{Nif}IscA.

For reaction times longer than 40 min, the spectrum of the $[4Fe\text{-}4S]^{2+}$ cluster broadens and decreases in intensity. Also, a broad and featureless spectrum extending from −4 mm/s to +5 mm/s develops (see Supporting Information, Figure S2). In correlation with the optical absorption study, this broad spectrum is assigned to polymeric iron sulfides

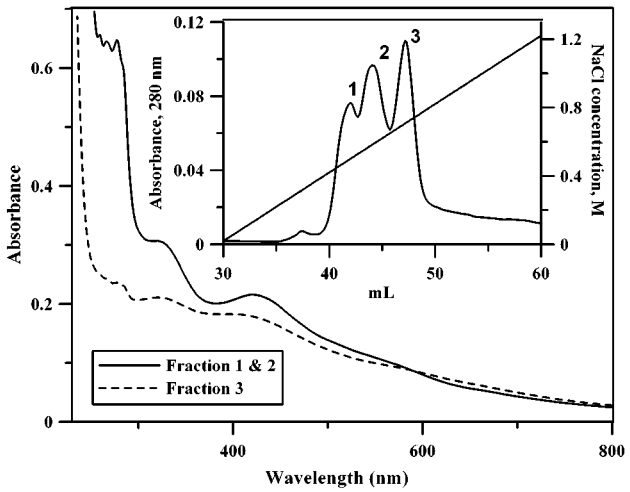

FIGURE 5: UV−vis absorption spectra of chromatographically resolved fractions of cluster-bound ^{Nif}IscA. Inset shows the elution profile of ^{Nif}IscA fractions contained in the NifS-catalyzed cluster assembly reaction mixture (see Materials and Methods). The reaction mixture was loaded anaerobically onto a 5-mL Q-sepharose column after a reaction time of 30 min. The absorption spectra correspond to fractions 1 and 2 (solid line) and fraction 3 (broken line) in an anaerobic 1 cm cuvette.

formed in solution. These observations indicate that the [4Fe-4S]$^{2+}$ cluster assembled in ^{Nif}IscA is unstable under the experimental conditions used.

To determine if NifS, cysteine, Fe(II), and ^{Nif}IscA constitute the minimum requirements for the assembly of a [4Fe-4S]$^{2+}$ cluster upon ^{Nif}IscA, Mössbauer spectroscopy was used to examine an array of controls in which NifS, ^{Nif}IscA, or NifS, and ^{Nif}IscA were omitted from the assembly cocktail. Formation of a [4Fe-4S]$^{2+}$ cluster was only detected in the control that included NifS, cysteine, and ferrous sulfate (see Supporting Information, Figure S1). In this case, less than 10% of the total Fe absorption was attributable to that of a [4Fe-4S]$^{2+}$ cluster, a result that is consistent with the previously recognized accumulation of self-assembled Fe−S clusters in anaerobic aqueous solution in the presence of sulfide, cysteine, and Fe(II) (*36*). However, incubation of the mixture without ^{Nif}IscA up to 40 min decreases the [4Fe-4S]$^{2+}$ cluster absorption to about 5%, rather than increasing to 42% as observed in the samples containing ^{Nif}IscA.

Purification and Characterization of Cluster-Containing Forms of ^{Nif}IscA. Attempts were made to separate apo ^{Nif}-IscA from cluster bound forms by using anion-exchange chromatography. In previous work (*15*), this approach was used successfully to separate apo IscU, IscU containing one [2Fe-2S]$^{2+}$ per dimer, IscU containing two [2Fe-2S]$^{2+}$ per dimer, and IscU containing one [4Fe-4S]$^{2+}$ cluster per dimer. Apo ^{Nif}IscA, however, has a considerably broader elution pattern when compared to IscU, eluting over a 20% NaCl gradient, compared with a gradient of less that 1% NaCl for each IscU isoform. Nevertheless, it was possible to achieve partial resolution of apo and cluster-bound forms of ^{Nif}IscA by anaerobic FPLC using a Q-Sepharose column (Figure 5). On the basis of the absorption characteristics, see above, the combined fractions 1 and 2 were shown to contain a mixture of apo and [2Fe-2S]$^{2+}$-bound forms of ^{Nif}IscA, whereas fraction 3 corresponds to [4Fe-4S]$^{2+}$-bound ^{Nif}IscA.

The [2Fe-2S]$^{2+}$-bound form was stable under anaerobic conditions and was further characterized by UV−vis absorption and resonance Raman spectroscopy (Figure 6), after further purification by anion-exchange chromatography and concentration using ultrafiltration. Iron analysis indicated 0.8 Fe/^{Nif}IscA monomer which corresponds to 0.8 [2Fe-2S]$^{2+}$ clusters/homodimeric ^{Nif}IscA. This result is consistent with the visible molar extinction coefficient at 415 nm, $\epsilon = 3.0$ mM^{-1} cm^{-1}, which also indicates approximately 0.4 [2Fe-2S]$^{2+}$ clusters/^{Nif}IscA monomer, based on the average value reported for well characterized 2Fe ferredoxins [$\epsilon_{420} \approx 8$ mM^{-1}cm^{-1} (*10*)]. Hence the purified sample contains approximately 1 [2Fe-2S]$^{2+}$/homodimeric ^{Nif}IscA. The resonance Raman spectrum in the Fe−S stretching region comprises an intense band at 289 cm^{-1} and additional bands at 337, 351, and 394 cm^{-1}. Although the possibility of one noncysteinyl ligand cannot be ruled out based solely on the Raman data, the vibrational frequencies and relative intensities of the Raman bands are characteristic of a protein-bound [2Fe-2S]$^{2+}$ cluster with complete cysteinyl ligation (*15*, *37*, *38*). The [4Fe-4S]$^{2+}$-bound form of ^{Nif}IscA was not stable even under strictly anaerobic conditions, and degraded to yield the soluble polymeric iron-sulfide species on standing a room temperature for 30 min or during concentration by ultrafiltration. Consequently, it has not yet been possible to obtain concentrated samples suitable for characterization by resonance Raman spectroscopy. No EPR signals indicative of a paramagnetic Fe−S cluster were observed in any of the cluster-bound forms of ^{Nif}IscA. Furthermore, the visible absorption of both the [2Fe-2S]$^{2+}$- and the [4Fe-4S]$^{2+}$-containing forms of ^{Nif}IscA were irreversibly and completely bleached on anaerobic reduction with dithionite or oxidation

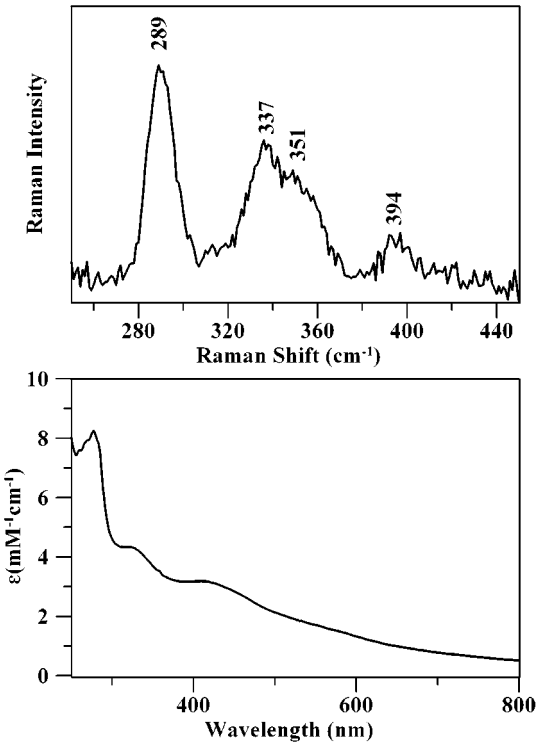

FIGURE 6: Resonance Raman and UV−vis absorption spectra of purified [2Fe-2S]$^{2+}$-containing form of ^{Nif}IscA. Upper panel: Raman spectrum at 17 K obtained with 457-nm excitation. The sample was ~2 mM in ^{Nif}IscA. The spectrum is the sum of 60 scans, with each scan involving photon counting for 1 s at 1-cm^{-1} increments, with 6 cm^{-1} resolution. Lower panel: Room-temperature absorption spectrum in a 1-cm cuvette. The sample was 0.12 mM in ^{Nif}IscA.

with ferricyanide, without the appearance of EPR signals indicative of any type of paramagnetic Fe−S cluster. Thus, the clusters in the $[2Fe\text{-}2S]^{2+}$- and the $[4Fe\text{-}4S]^{2+}$-containing forms of ^{Nif}IscA are both oxidatively and reductively labile.

DISCUSSION

The results presented in this work show that *A. vinelandii* ^{Nif}IscA does not bind Fe(III) ion and has only a weak affinity for binding Fe(II) ion in a tetrahedral, predominantly cysteinyl-ligated coordination environment. Hence, a role for IscA proteins in delivering iron to cluster assembly proteins seems unlikely. The possibility of this type of "iron chaperone" role was previously suggested for the equivalent Isa1p and Isa2p proteins in *S. cerevisiae* on the basis of genetic and cellular location arguments (*19*). However, the location of Isa2p in the mitochondrial intermembrane space has since been questioned by Lill and co-workers (*20*), and a location in the matrix space along with all the other proteins involved with eukaryotic Fe−S cluster biosynthesis makes a role involving Fe or Fe−S cluster transport less appealing. Moreover, the results presented herein show that ^{Nif}IscA provides an alternative scaffold to NifU[3] for the NifS-directed assembly of the $[4Fe\text{-}4S]^{2+}$ clusters that are involved in the maturation of the nitrogenase component proteins. By analogy, we propose that IscA-type proteins in both prokaryotic and eukaryotic organisms could serve as alternative scaffolds to the IscU-type proteins (*15*) in the IscS-directed assembly of $[4Fe\text{-}4S]^{2+}$ and/or $[2Fe\text{-}2S]^{2+}$ clusters necessary for general maturation of Fe−S proteins.

The proposal that IscA-type proteins provide an alternative scaffold to the IscU-type proteins for Fe−S cluster biosynthesis is consistent with the available genetic evidence that demonstrates an important but nonessential role for IscA in Fe−S cluster biosynthesis. Studies using *S. cerevisiae* have shown that the two ^{Nif}*iscA* homologues, *ISA1* and *ISA2*, have a nonredundant function as knockouts to either or both have the same phenotype, i.e., retarded growth on nonfermentable carbon source, accumulation of iron in mitochondria, and marked decrease in the activities of mitochondrial and cytosolic Fe−S enzymes (*19*−*21*). In contrast, a knockout to both *iscu* homologues in *S. cerevisiae*, *ISU1* and *ISU2*, is lethal (*39*). Studies in *E. coli* have also indicated an important role for IscA in de novo Fe−S cluster biosynthesis (*17*, *18*). However, in contrast to *S. cerevisiae*, the genes in the *isc* operon are necessary for optimal growth but are not essential for the viability of *E. coli* cells (*18*, *40*), suggesting the presence of a redundant system for Fe−S cluster biosynthesis. Nevertheless, the phenotypical consequences of inactivation of the *E. coli IscA* genes in terms of growth rate, nutritional requirements and activities of Fe−S enzymes, were significant, but much less pronounced than for inactivation of *iscS*, *iscU*, *hscA*, *hscB*, or *fdx* (*18*).

The spectroscopic and analytical results indicate that NifS-directed cluster assembly on ^{Nif}IscA proceeds via an intermediate involving approximately one $[2Fe\text{-}2S]^{2+}$ cluster per homodimer to yield a final product involving approximately one labile $[4Fe\text{-}4S]^{2+}$ cluster per homodimer. Sequential assembly of $[2Fe\text{-}2S]^{2+}$ clusters leading to formation of one $[4Fe\text{-}4S]^{2+}$ per homodimer was also observed for IscS-mediated cluster assembly on IscU (*15*). In this case, a tentative mechanism involving reductive coupling of two $[2Fe\text{-}2S]^{2+}$ clusters to yield a single $[4Fe\text{-}4S]^{2+}$ has been proposed (*12*). However, the cluster assembly processes on IscU and ^{Nif}IscA appear to exhibit some significant differences. First, there is no evidence for an intermediate species involving two $[2Fe\text{-}2S]^{2+}$ clusters per homodimer during cluster assembly on ^{Nif}IscA. However, this observation does not necessarily demonstrate that $[4Fe\text{-}4S]^{2+}$ cluster assembly proceeds by a different mechanisms on the ^{Nif}IscA and IscU scaffolds nor does it preclude the existence of a stable form of ^{Nif}IscA containing two $[2Fe\text{-}2S]^{2+}$ cluster per homodimer. Rather, it might simply reflect a faster reductive coupling step during NifS-catalyzed cluster assembly on ^{Nif}IscA, compared to IscS-catalyzed cluster assembly on IscU, resulting in no significant accumulation of an intermediate containing two $[2Fe\text{-}2S]^{2+}$ clusters per ^{Nif}IscA homodimer. Second, the Mössbauer and resonance Raman characteristics of the $[2Fe\text{-}2S]^{2+}$ cluster assembled on ^{Nif}IscA are best interpreted in terms of complete cysteinyl ligation, whereas the two identical $[2Fe\text{-}2S]^{2+}$ clusters that can be assembled on homodimeric IscU have at least one noncysteinyl ligand as evidenced by the spectroscopic characteristics and the availability of only six cysteine residues (*12*, *15*).

Marked differences are apparent in the spectroscopic properties of the $[2Fe\text{-}2S]^{2+}$ clusters assembled on IscU and ^{Nif}IscA. The two antiferromagnetically coupled high-spin Fe(III) sites of the ^{Nif}IscA $[2Fe\text{-}2S]^{2+}$ cluster exhibit identical isomer shifts ($\delta = 0.26$ mm/s) and quadrupole splittings ($\Delta E_Q = 0.55$ mm/s) and both are characteristic of tetrahedral sulfur coordination, i.e., complete cysteinyl ligation. In contrast, the two high-spin Fe(III) sites of the IscU $[2Fe\text{-}2S]^{2+}$ cluster have quite distinct Mössbauer parameters, $\delta = 0.26$ mm/s and $\Delta E_Q = 0.64$ mm/s for site 1 and $\delta = 0.32$ mm/s and $\Delta E_Q = 0.91$ mm/s for site 2 (*15*). While the parameters for site 1 are indicative of two terminal cysteine ligands, those for site 2 are indicative of one or possibly two noncysteine ligands (*15*). The resonance Raman spectra of the $[2Fe\text{-}2S]^{2+}$ clusters assembled on IscU and ^{Nif}IscA, obtained with 457-nm excitation (cf. Figure 6 and Figure 3 of ref *15*), are similar in terms of the relative intensities of the major bands, but the equivalent bands are shifted to much lower frequencies (major bands at 289, 337, 351, and 394 cm^{-1} in ^{Nif}IscA compared to 296, 356, 370, and 407 cm^{-1} in IscU). The frequency shifts can be interpreted in terms of $[2Fe\text{-}2S]^{2+}$ clusters with the same ligation, but with weaker Fe−S(bridging) and Fe−S(Cys) bonds for ^{Nif}IscA compared to IscU, or complete cysteinyl ligation for the $[2Fe\text{-}2S]^{2+}$ cluster in ^{Nif}IscA. The frequencies of the A_gt and B_{3u}t Fe−S stretching modes have been shown to be sensitive to replacing a coordinated cysteine by an oxygenic ligand (*15*, *38*). These modes occur at 289 and 337 cm^{-1}, respectively (compared to 296 and 356 cm^{-1}, respectively in IscU), and lie within the range established for clusters with complete cysteinyl ligation [281−291 and 326−340 cm^{-1}, respectively (*15*, *38*)]. Taken together, the Mössbauer and resonance Raman results are most reasonably interpreted in terms of

[3] The published spectroscopic studies on a truncated form of NifU and variant forms of holo NifU have provided evidence for NifS-directed assembly of a transient $[2Fe\text{-}2S]^{2+}$ cluster in the N-terminal IscU-like domain. However, recent Mössbauer studies of NifS-directed cluster assembly on wild-type natural abundance holo-NifU using ^{57}Fe ferric ammonium citrate, have shown that a $[4Fe\text{-}4S]^{2+}$ cluster is the final product of cluster assembly at the IscU-like domain (Agar, J. N., Smith, A. D., Krebs, C., Frazzon, J., Dean, D. R., Huynh, B. H., and Johnson, M. K., manuscript in preparation).

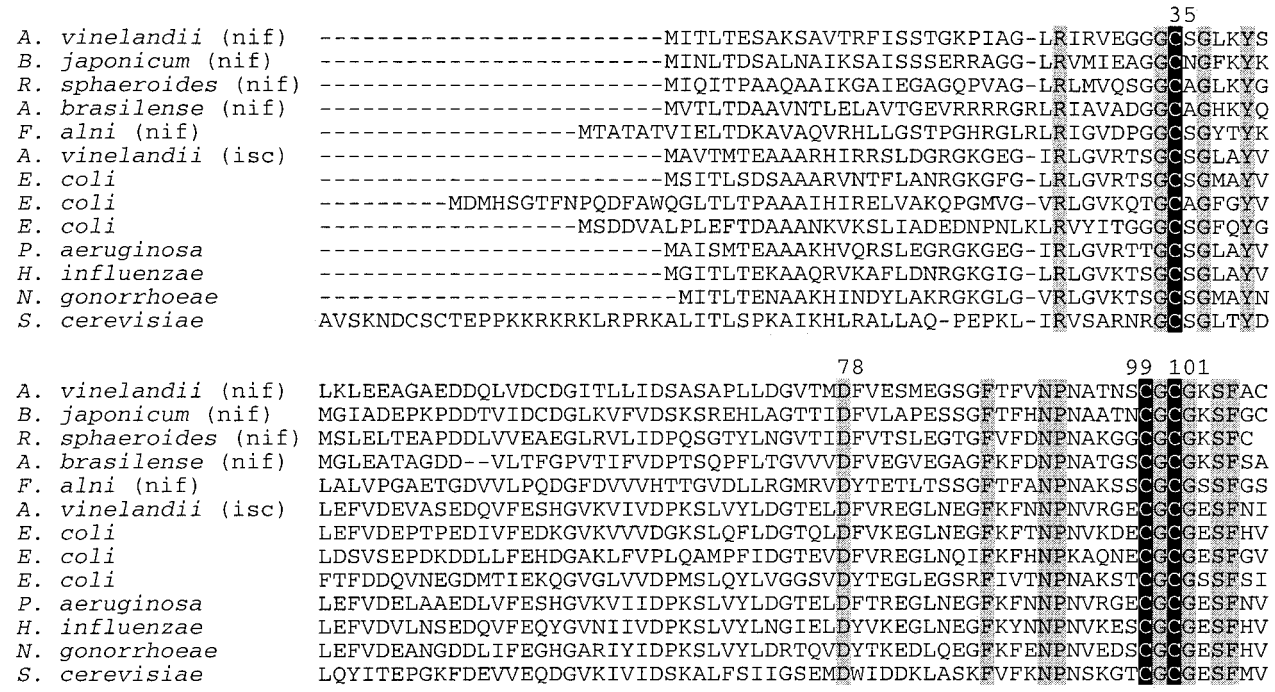

FIGURE 7: Primary sequence alignments for IscA proteins. Light shading indicates identical residues and dark shading indicates conserved cysteines. The numbers correspond to strictly conserved cysteine and aspartate residues in *A. vinelandii* IscA and ^{Nif}IscA.

complete cysteinyl ligation for the $[2Fe\text{-}2S]^{2+}$ cluster assembled in ^{Nif}IscA. However, it is not possible to rule out a coordination environment involving three cysteinate and one oxygenic ligand based on the available spectroscopic results.

The best candidates for iron or cluster binding residues in IscA proteins are the three conserved cysteines (residues 35, 99, and 101 in *A. vinelandii* IscA and ^{Nif}IscA) and a conserved aspartate (residue 78 in *A. vinelandii* IscA and ^{Nif}IscA). These residues are conserved among all IscA type proteins from prokaryotic and eukaryotic organisms, including all known *nif*-specific IscA proteins (Figure 7). Moreover, individual amino acid substitutions for each of the three conserved cysteine residues of the yeast Isa1p and Isa2p proteins (IscA homologues) yield the same phenotypes as the gene knockouts (*19*, *21*). The available mutagenesis evidence for NifU suggests the involvement of a conserved aspartate in cluster ligation in NifU and IscU proteins (*12*), which leads to a primary sequence arrangement of C−G−D−X_{22-24}−C−X_{43}−C for the putative cluster binding residues in IscU. In light of the similar roles for IscU and IscA proteins, it may be relevant to note that a similar spatial arrangement is essentially preserved in IscA proteins, C−X_{42}−D−X_{20}−C−G−C, albeit reversed and with a different placement of the aspartate residue.

In addition to the three cysteines conserved in all IscA-type proteins, *A. vinelandii* ^{Nif}IscA contains two other cysteines, one at the residue 57 position and the other at the C-terminus. However, these cysteines are not conserved in all ^{Nif}IscA proteins (Figure 7) and are therefore unlikely to be mononuclear iron or Fe−S cluster ligands. For the mononuclear Fe(II) site, tetrahedral coordination by three cysteinate and one oxygenic ligand is entirely consistent with the UV absorption and VTMCD data. Moreover, such coordination scheme is further supported by the observation of identical UV absorption and VTMCD data for the Fe(II)-bound form of the general IscA protein from *A. vinelandii*,[4] which has only the three conserved cysteine residues and no others (Figure 7). However, complete cysteinyl ligation for the $[2Fe\text{-}2S]^{2+}$ cluster using only the conserved cysteines on ^{Nif}IscA necessitates a subunit-bridging arrangement. Mutagenesis and more definitive structural studies are clearly required to identify the specific ligands and the location of clusters assembled on IscA-type proteins.

The results reported in this work have important mechanistic implications for the NifS/IscS-directed assembly of Fe−S clusters on scaffold proteins. Although NifS- or IscS-directed Fe−S cluster assembly has been reported for NifU (*11*, *12*) and IscU (*14*, *15*), and sequential formation of $[2Fe\text{-}2S]^{2+}$ and $[4Fe\text{-}4S]^{2+}$ clusters has been reported for IscU (*15*), the procedure used in the present work differs in two important respects. First, ferrous sulfate rather than ferric ammonium citrate was used as the iron source. However, ferric ion in solution at pH 7.8 has been shown to be reduced by excess cysteine to yield ferrous ion and cystine (*41*) and this was confirmed by Mössbauer experiments under the conditions used in the cluster assembly experiments (data not shown). Hence, ferrous ion rather than ferric ion is utilized for NifS- or IscS-mediated cluster assembly on the both types of scaffold protein. Second, in all previous studies, a reductant, such as β-mercaptoethanol or dithiothreitol, which is capable of mediating sulfide release from a NifS- or IscS-associated cysteine persulfide (*9*, *42*), was present in the reaction mixture. In the current work, neither β-mercaptoethanol nor dithiothreitol was added to the cluster assembly cocktail. Also, it is unlikely that cysteine (which is present in this study) could be a direct source of electrons for the liberation of sulfide from NifS, as the rate of this reaction is 2 orders of magnitude below that of sulfide production required for the rapid formation of $[2Fe\text{-}2S]^{2+}$

[4] Agar, J. N., Frazzon, J., Dean, D. R., and Johnson, M. K., unpublished results.

Scheme 1

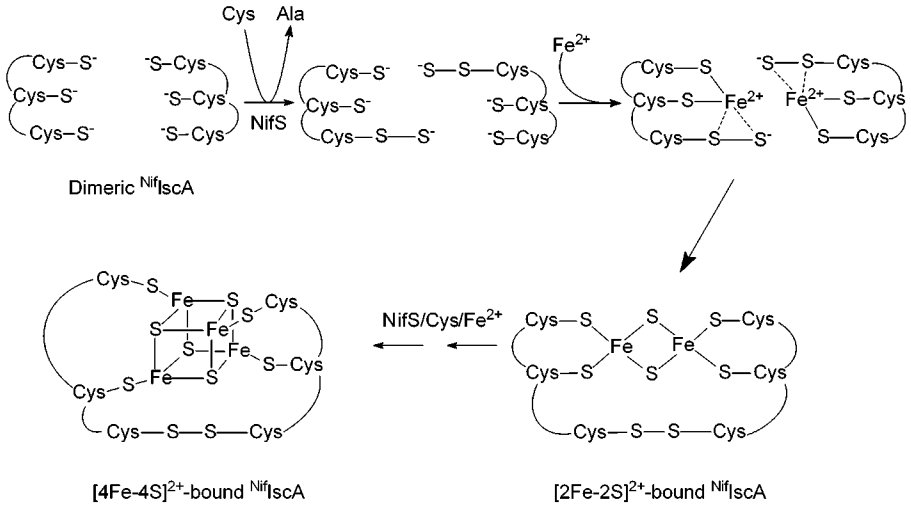

Scheme 2

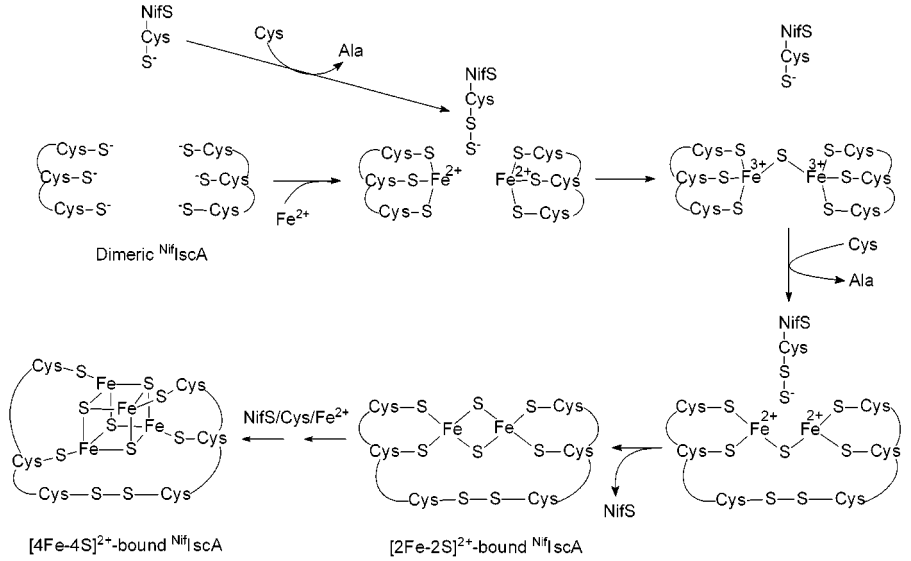

clusters observed in this work (*9*, *42*). Thus, ferrous ion must provide the reducing equivalents, in whole or in part, for the reduction of a cysteine persulfide to yield sulfide.

To understand the reaction mechanism, it is important to consider the stoichiometries of reactants and products. For the observed sequential formation of $[2Fe\text{-}2S]^{2+}$ and $[4Fe\text{-}4S]^{2+}$ clusters during the cluster assembly process, the reaction stoichiometry may be summarized by the following two equations:

$$2Fe^{2+} + 2S^0 + 2e^- \rightarrow [2Fe\text{-}2S]^{2+} \quad (1)$$

$$2[2Fe\text{-}2S]^{2+} + 2e^- \rightarrow [4Fe\text{-}4S]^{2+} \quad (2)$$

In eq 1, S° represents the inorganic sulfur of a bound cysteine-persulfide that must be reduced to S^{2-} for cluster formation. According to the Mössbauer data, only $[2Fe\text{-}2S]^{2+}$, $[4Fe\text{-}4S]^{2+}$, and Fe(II) species were present in the reaction mixture during the cluster assembly process. Mononuclear Fe(III) species were not detected. Coupled with the fact that the formation of a $[2Fe\text{-}2S]^{2+}$ cluster involves the oxidation of two ferrous ions, the observation that no mononuclear Fe(III) species are observed dictates that the electrons required for the reduction of S° to S^{2-} must be derived from the ferrous ions that form the $[2Fe\text{-}2S]^{2+}$ cluster. In other words, the two processes required for cluster assembly, namely oxidation of iron and reduction of cysteine persulfide, appear to be coupled. On the other hand, a $[2Fe\text{-}2S]^{2+}$ cluster contains two sulfide anions. Consequently, the formation of one $[2Fe\text{-}2S]^{2+}$ cluster requires four electrons for the production of two sulfides. Since the oxidation of the two ferrous ions can only provide half the necessary electrons, two additional electrons are required for the formation of a $[2Fe\text{-}2S]^{2+}$ cluster (eq 1). These two electrons must come from either the oxidation of cysteine residues on ^{Nif}IscA to form a cysteine disulfide or the oxidation of exogenous cysteine to form cystine. On the basis of these considerations and the ligation and stoichiometries of the assembled clusters, see above, two alternative mechanisms (Schemes 1 and 2) are proposed for the formation of the transient $[2Fe\text{-}2S]^{2+}$ cluster on ^{Nif}IscA. Both are offered as working hypotheses designed to stimulate future experiments.

The schemes differ primarily in terms of the initial step of cluster assembly, i.e., sulfur transfer from NifS or Fe(II) ion binding to ^{Nif}IscA. In Scheme 1, the first step is sulfur

transfer from NifS to create a cysteine persulfide on each ^{Nif}IscA monomer. Precedent for transfer of a sulfane sulfur from a cysteine persulfide on IscS protein to form a cysteine persulfide at the active site cysteine of an acceptor protein is provided by ThiI (*43*). Moreover, direct transfer of sulfane sulfur from IscS to the cysteine residues on IscU has recently been demonstrated using mass spectrometry (*44*). This transfer is followed by Fe(II) binding to the cysteinyl sulfurs and both sulfurs of the cysteine persulfide of each ^{Nif}IscA monomer. Formation of a cysteinyl-ligated $[2Fe\text{-}2S]^{2+}$ cluster then occurs at the subunit interface via a concerted mechanism, with oxidation of the two ferrous ions and formation of intersubunit disulfide providing the four electrons required for the reduction of two sulfane sulfurs to sulfides. In scheme 2, the first step involves ferrous binding to ^{Nif}IscA in a ^{Nif}IscA/NifS complex. Although ^{Nif}IscA has been shown to have a weak affinity for binding ferrous ion, it has yet to be determined if the binding affinity is enhanced by the addition of cysteine-pretreated NifS in a 1:1 stoichiometry. The reaction then proceeds in two steps with the first involving reductive cleavage of the cysteine persulfide on NifS to yield a sulfide-bridged diferric species. This process is then repeated following reduction of the diferric center via the formation of an intersubunit disulfide to yield a subunit-bridging cysteinyl-ligated $[2Fe\text{-}2S]^{2+}$ cluster.

On the basis of the observation that $[4Fe\text{-}4S]^{2+}$ clusters accumulate following the formation of $[2Fe\text{-}2S]^{2+}$ clusters and that the $[2Fe\text{-}2S]^{2+}$ cluster is transient, it is proposed that the formation of a $[4Fe\text{-}4S]^{2+}$ cluster results from reductive coupling of two $[2Fe\text{-}2S]^{2+}$ clusters as depicted in eq 2. The overall reaction of combining two $[2Fe\text{-}2S]^{2+}$ clusters to form a $[4Fe\text{-}4S]^{2+}$ cluster requires two electrons, since a $[2Fe\text{-}2S]^{2+}$ cluster is comprised of two Fe(III) ions whereas a $[4Fe\text{-}4S]^{2+}$ cluster contains two mixed-valent Fe(II)/Fe(III) pairs. In our reaction mixture, these electrons are most likely ultimately derived from oxidation of exogenous cysteine to cystine. In the current models, the second $[2Fe\text{-}2S]^{2+}$ cluster would form at the subunit interface with two noncysteinyl ligands and assembly would be initiated by cysteine cleavage of the intersubunit disulfide. Subsequent reformation of this disulfide would then provide the electrons for the reductive coupling process depicted in eq 2. In both schemes, reduction of the intersubunit disulfide would provide an attractive method for reductive release of $[2Fe\text{-}2S]^{2+}$ or $[4Fe\text{-}4S]^{2+}$ clusters destined for insertion in to apo Fe−S proteins. It should be pointed out, however, that the process described in eq 2 is very complex, involving the formation and cleavage of many Fe−ligand bonds. Kinetic and spectroscopic characterization of reaction intermediates will be required for mechanistic understanding. Thus, formulation of a mechanistic scheme has not been attempted. Temporal information has been obtained in this work, but the study was performed under steady state conditions. Under such conditions, accumulation of kinetically competent intermediates is not possible. The observed accumulation of $[2Fe\text{-}2S]^{2+}$- and $[4Fe\text{-}4S]^{2+}$-bound forms of ^{Nif}IscA clusters indicates that they represent thermodynamically stable products rather then reaction intermediates.

While this manuscript was in preparation, a manuscript was published on *E. coli* IscA (*45*). Evidence was presented for the assembly of one $[2Fe\text{-}2S]^{2+}$ cluster per IscA polypeptide, using standard cluster reconstitution conditions (anaerobic addition of ferrous sulfate and sodium sulfide in the presence of DTT), and for the formation of a complex between cluster-bound IscA and Fdx, the prokaryotic homologue of Yah1p [2Fe-2S] ferredoxin in yeast. The observation that only the cluster-bound IscA was capable of forming a complex with Fdx, coupled with apparent observation of cluster transfer from cluster-bound IscA to apo Fdx, led to the proposal that IscA is a specific scaffold protein for the assembly of clusters on Fdx. These results are quite different from those obtained in this work and, taken at face value, would suggest that reconstituted IscA and ^{Nif}IscA differ in terms of the number and type of the assembled Fe−S clusters.

We have considered several ways of reconciling the results reported for *E. coli* IscA with those obtained herein for *A. vinelandii* ^{Nif}IscA. First, it is possible that ^{Nif}IscA is specific for the assembly of $[4Fe\text{-}4S]^{2+}$ clusters, whereas general IscA proteins are specific for assembly of $[2Fe\text{-}2S]^{2+}$ clusters or cluster fragments. Second, the nature of the cluster assembled on IscA-type proteins may depend on the assembly protocol used. Using the physiological sulfur donor, i.e., cysteine and IscS or NifS, the sulfur is presented as S°, as opposed to S^{2-} in the standard in vitro reconstitution procedure, and this might alter the number and type of clusters assembled. Third, it is possible that $[4Fe\text{-}4S]^{2+}$ clusters can be assembled on *E. coli* IscA using standard in vitro reconstitution conditions but were not detected due to instability or the spectroscopic/analytical techniques employed in the published work (*45*). In this connection, it is important to note that $[2Fe\text{-}2S]^{2+}$-bound ^{Nif}IscA was found to be more stable under anaerobic conditions than $[4Fe\text{-}4S]^{2+}$-bound ^{Nif}IscA. In addition, the conclusion that one $[2Fe\text{-}2S]^{2+}$ cluster can be assembled on each *E. coli* IscA polypeptide was based solely on UV−vis absorption spectra and iron/sulfide analysis of samples purified using a Sephadex G-25 column, a procedure that in our experience does not remove the soluble polymeric iron-sulfides that are present in solution and contribute absorption bands at 420 and 600 nm (see Figure 2, broken line). The presence of polymeric iron-sulfides would conceal the presence of $[4Fe\text{-}4S]^{2+}$ clusters in the absorption spectrum and lead to overestimates of protein-associated iron and acid-labile sulfur. Finally, in the presence of $[2Fe\text{-}2S]^{2+}$ clusters, the detection of $[4Fe\text{-}4S]^{2+}$ clusters by resonance Raman spectroscopy may be difficult due to the fact that resonance enhancements of the Fe−S stretching modes of $[4Fe\text{-}4S]^{2+}$ clusters are at least an order of magnitude less than that of $[2Fe\text{-}2S]^{2+}$ clusters using 496-nm excitation.

The published results for *E. coli* IscA provide convincing evidence for a complex between cluster-bound IscA and Fdx (*45*). However, the evidence for cluster transfer from *E. coli* IscA to apo Fdx (*45*) is less compelling, because the absorption spectrum of the cluster-bound IscA used in these experiments appears to have a significant contribution from non-protein-associated soluble iron-sulfides. A specific role for IscA in cluster assembly on Fdx also seems unlikely based on genetic evidence. For example, the Isap proteins in yeast cannot be solely responsible for the cluster assembly of the ferredoxin homologue, Yah1p, as knockouts of Yah1p are lethal (*46*), whereas Isa knockouts are not (*19*−*21*). Likewise, in the case of *E. coli*, inactivation of Fdx results in a much more severe phenotype than inactivation of IscA (*18*). In our view, complex formation between Fdx and IscA

is more likely to relate to an electron transfer event necessary for efficient cluster assembly or release.

The above discussion serves to underscore the need for further cluster assembly and transfer experiments with both ^{Nif}IscA and IscA proteins. Nevertheless, both the present study and the work of Ollagnier-de-Choudens et al. (*45*) are consistent with a role for IscA-type proteins as an alternative scaffold to IscU-type proteins for IscS-mediated cluster assembly.

This work and our previous studies of *A. vinelandii* NifU and IscU (*11*, *12*, *14*, *15*) have demonstrated the use of scaffold proteins for Fe−S cluster biosynthesis. Aside from the obvious advantage of having a ready-made cluster to insert, this work serves to highlight another important advantage of the use of a scaffold protein, namely the ability of ^{Nif}IscA to couple ferrous ion oxidation with S° reduction. This feature results in a situation where S^{2-} formation can be controlled by iron availability, thereby preventing the deleterious accumulation of free S^{2-} in the cell. Moreover, subsequent experiments have shown that the previously described scaffold proteins, IscU and NifU, are also effective in coupling iron and sulfur delivery.[5] One important question that remains to be answered is why alternative scaffold proteins are involved, because both IscA- and IscU-type proteins are present in most organisms. Some plausible reasons for the need for alternative scaffolds are that IscA and IscU are optimized for assembly of either $[2Fe\text{-}2S]^{2+}$ or $[4Fe\text{-}4S]^{2+}$ clusters in vivo, that each preferentially transfer clusters to different acceptor proteins, or that each functions optimally under different physiological conditions. In vivo and in vitro studies are planned to address these issues and to elucidate the detailed mechanism of cluster assembly and release in both types of scaffold protein. Future studies will also assess the benefits of scaffold proteins by developing a functional in vitro assay for scaffold-assisted insertion of Fe−S clusters into apo Fe−S proteins.

SUPPORTING INFORMATION AVAILABLE

Mössbauer spectra of control samples (Figure S1) and the Mössbauer spectrum of a sample frozen at a reaction time of 4 h during the reaction of NifS-catalyzed assembly of Fe−S cluster on ^{Nif}IscA (Figure S2). This material is available free of charge via the Internet at http://pubs.acs.org.

REFERENCES

1. Johnson, M. K. (1994) in *Encyclopedia of Inorganic Chemistry* (King, R. B., Ed.) pp 1896−1915, John Wiley & Sons, Chichester, U.K.
2. Beinert, H., Holm, R. H., and Münck, E. (1997) *Science 277*, 653−659.
3. Johnson, M. K. (1998) *Curr. Opin. Chem. Biol. 2*, 173−181.
4. Beinert, H., and Kiley, P. J. (1999) *Curr. Opin. Chem. Biol. 3*, 152−157.
5. Beinert, H. (2000) *J. Biol. Inorg. Chem. 5*, 2−15.
6. Jacobson, M. R., Cash, V. L., Weiss, M. C., Laird, N. F., Newton, W. E., and Dean, D. R. (1989) *Mol. Gen. Genet. 219*, 49−57.
7. Dean, D. R., Bolin, J. T., and Zheng, L. (1993) *J. Bacteriol. 175*, 6737−6744.
8. Zheng, L., White, R. H., Cash, V. L., Jack, R. F., and Dean, D. R. (1993) *Proc. Natl. Acad. Sci. U.S.A. 90*, 2754−2758.
9. Zheng, L., White, R. H., Cash, V. L., and Dean, D. R. (1994) *Biochemistry 33*, 4714−4720.
10. Fu, W., Jack, R. F., Morgan, T. V., Dean, D. R., and Johnson, M. K. (1994) *Biochemistry 33*, 13455−13463.
11. Yuvaniyama, P., Agar, J. N., Cash, V. L., Johnson, M. K., and Dean, D. R. (2000) *Proc. Natl. Acad. Sci. U.S.A. 97*, 599−604.
12. Agar, J. N., Dean, D. R., and Johnson, M. K. (2001) in *Biochemistry and Physiology of Anaerobic Bacteria* (Ljungdahl, L. G., Adams, M. W. W., Barton, L. L., Ferry, J. G., and Johnson, M. K., Eds.) Springer-Verlag, New York (in press).
13. Zheng, L., Cash, V. L., Flint, D. H., and Dean, D. R. (1998) *J. Biol. Chem. 273*, 13264−13272.
14. Agar, J. N., Zheng, L., Cash, V. L., Dean, D. R., and Johnson, M. K. (2000) *J. Am. Chem. Soc. 122*, 2136−2137.
15. Agar, J. N., Krebs, B., Frazzon, J., Huynh, B. H., Dean, D. R., and Johnson, M. K. (2000) *Biochemistry 39*, 7856−7862.
16. Lill, R., and Kispal, G. (2000) *Trends Biochem. Sci. 25*, 352−356.
17. Takahashi, Y., and Nakamura, M. (1999) *J. Biochem. 126*, 917−926.
18. Tokumoto, U., and Takahashi, Y. (2001) *J. Biochem. 130*, 63−71.
19. Jensen, L. T., and Culotta, V. C. (2000) *Mol. Cell. Biol. 20*, 3918−3927.
20. Pelzer, W., Mühlenhoff, U., Diekert, K., Siegmund, K., Kispal, G., and Lill, R. (2000) *FEBS Lett. 476*, 134−139.
21. Kaut, A., Lange, H., Diekert, K., Kispal, G., and Lill, R. (2000) *J. Biol. Chem. 275*, 15955−15961.
22. Brown, R. E., Jarvis, K. L., and Hyland, K. J. (1989) *Anal. Biochem. 180*, 136−139.
23. Haigler, B. E., and Gibson, D. T. (1990) *J. Bacteriol. 172*, 457−464.
24. Drozdzewski, P. M., and Johnson, M. K. (1988) *Appl. Spectrosc. 42*, 1575−1577.
25. Johnson, M. K. (2000) in *Physical Methods in Bioinorganic Chemistry. Spectroscopy and Magnetism* (Que, L., Jr., Ed.) pp 233−286, University Science Books, Sausilito, CA.
26. Thomson, A. J., Cheesman, M. R., and George, S. J. (1993) *Methods Enzymol. 226*, 199−232.
27. Ravi, N., Bollinger, J. M., Huynh, B. H., Edmondson, D. E., and Stubbe, J. (1994) *J. Am. Chem. Soc. 116*, 8007−8014.
28. Werth, M. T., and Johnson, M. K. (1989) *Biochemistry 28*, 3982−3988.
29. Bennett, D. E., and Johnson, M. K. (1987) *Biochim. Biophys. Acta 911*, 71−80.
30. Huynh, B. H., and Kent, T. A. (1984) *Adv. Inorg. Biochem. 6*, 163−223.
31. Staples, C. R. (1997) Ph. D. dissertation, University of Georgia.
32. Dailey, H. A., Finnegan, M. G., and Johnson, M. K. (1994) *Biochemistry 33*, 403−407.
33. Greenwood, N. N., and Gibb, T. C. (1971) *Mössbauer Spectroscopy*, Chapman and Hall, London, U.K.
34. Que, L., Jr. (1983) *Coord. Chem. Rev. 50*, 73−108.
35. Tavares, P., Ravi, N., Moura, J. J. G., LeGall, J., Huang, Y.-H., Crouse, B. R., Johnson, M. K., Huynh, B. H., and Moura, I. (1994) *J. Biol. Chem. 269*, 10504−10510.
36. Holm, R. H. (1977) *Acc. Chem. Res. 10*, 427−434.
37. Han, S., Czernuszewicz, R. S., Kimura, T., Adams, M. W. W., and Spiro, T. G. (1989) *J. Am. Chem. Soc. 111*, 3505−3511.
38. Crouse, B. R., Sellers, V. M., Finnegan, M. G., Dailey, H. A., and Johnson, M. K. (1996) *Biochemistry 35*, 16222−16229.
39. Schilke, B., Voisine, C., Beinert, H., and Craig, E. (1999) *Proc. Natl. Acad. Sci. U.S.A. 96*, 10206−10211.
40. Schwartz, C. J., Djaman, O., Imlay, J. A., and Kiley, P. J. (2000) *Proc. Natl. Acad. Sci. U.S.A. 97*, 9009−9014.
41. Jameson, R. F., Linert, W., and Tschinkowitz, A. (1998) *J. Chem. Soc., Dalton Trans.* 2109−2112.
42. Flint, D. H. (1996) *J. Biol. Chem. 271*, 16068−16074.
43. Kambampati, R., and Lauhon, C. T. (2000) *J. Biol. Chem. 275*, 10727−10730.

[5] Agar, J. N., Smith, A. D., Krebs, C., Frazzon, J., Dean, D. R., Huynh, B. H., and Johnson, M. K, unpublished results.

44. Smith, A. D., Agar, J. N., Johnson, K. A., Frazzon, J., Amster, I. J., Dean, D. R., and Johnson, M. K. (2001) *J. Am. Chem. Soc.* (in press).
45. Ollagnier-de-Choudens, S., Mattioli, T., Takahashi, Y., and Fontecave, M. (2001) *J. Biol. Chem. 276*, 22604−22607.
46. Lange, H., Kaut, A., Kispal, G., and Lill, R. (2000) *Proc. Natl. Acad. Sci. U.S.A. 97*, 1050−1055.

BI015656Z